Acta Cryst. (1970). B**26**, 1010

An Electron Diffraction Study of the Structures of Thiophene, 2-Chlorothiophene and 2-Bromothiophene

BY W. R. HARSHBARGER* AND S. H. BAUER

Department of Chemistry, Cornell University, Ithaca, New York 14850, *U.S.A.*

(*Received* 7 *April* 1969)

The structures of thiophene, 2-chlorothiophene and 2-bromothiophene were determined by gas phase electron diffraction. Two sets of sectored diffraction patterns of thiophene were recorded; their ranges were $6 \le q \le 120$ Å^{-1} and $6 \le q \le 125$ Å^{-1}. The molecular intensity functions for the two sets of data for thiophene were fitted independently by least-squares analyses to give; C–S$=1{\cdot}717 \pm 0{\cdot}004$, C=C$=1{\cdot}368 \pm 0{\cdot}004$, C–H$=1{\cdot}071 \pm 0{\cdot}015$ Å, $\angle$CSC$=91{\cdot}9 \pm 0{\cdot}30$, $\angle$SCC$=111{\cdot}9 \pm 0{\cdot}3$, $\angle$SCH$=121 \pm 3$, $\angle$C(3)C(4)H$=120 \pm 6°$. The diffraction pattern for 2-chlorothiophene was analyzed over the range of $3 \le q \le 115$ Å^{-1} and for 2-bromothiophene over the range of $4 \le q \le 119$ Å^{-1}. Least-squares analyses of the molecular intensity functions indicated that two significantly different structures fitted the data equally well for each of these derivatives. However, other physical and chemical evidence favors those models for the halogenated thiophenes in which the bonds adjacent to the halogen atom are lengthened and the bonds across the ring are shortened relative to the analogous bond lengths in thiophene. This distortion is attributed to inductive and mesomeric effects of the halogen upon the thiophene moiety. For all three molecules the best models are planar.

Introduction

Many of the physical and chemical properties of thiophene are attributable to electron delocalization of the π-system of the planar ring. Longuet-Higgins (1949) accounted for the ultraviolet spectrum of thiophene and for the relative reactivity at the α and β carbon atoms on the basis of molecular orbital calculations. In his analysis, the sulfur atom in the ring contributes two electrons to the π-bonding system, giving thiophene aromatic character, similar to benzene. The observed C–C and C–S bond lengths in previous structure determinations of thiophene by Bak, Christensen, Hansen-Nygaard & Rastrup-Andersen (1961) and Bonham & Momany (1963) support the postulate that in the ring some electron delocalization does occur. Also, one may underscore the similarity of the physical and chemical properties of thiophene and benzene.

One of the interesting properties of benzene which has been noted by chemists is the immutability of the benzene ring geometry upon substitution. An example of this property was demonstrated by Bauer, Katada & Kimura (1968) in their study of hexafluorobenzene and *S*-trifluorobenzene. Their results, along with gas-phase structure determinations of bromobenzene, fluorobenzene, phenyl cyanide, perchlorobenzene, 1,2,4,5-tetrachlorobenzene and 1,2,4,5-tetrabromobenzene, as reported in the literature, led to the conclusions that the carbon skeleton retains its D_{6h} symmetry, and that the hexagon remains to within $\pm 0{\cdot}005$ Å of the size found in benzene, 1·397 Å (Almenningen, Bastiansen & Fernholt, 1958; Langseth & Stoicheff, 1956; Kimura & Kubo, 1960).

Structure determinations of cyanuric trifluoride (Bauer *et al.*, 1968), cyanuric trichloride and *s*-triaminotriazene (Akimoto, 1955) indicate that for these symmetric substitutions the C–N bond distance retains, within experimental error ($\pm 0{\cdot}01$ Å), the value reported for *s*-triazene, $1{\cdot}338 \pm 0{\cdot}001$ Å (Lancaster & Stoicheff, 1956). This suggests that the aromatic *s*-triazene ring is also undistorted by substitutions.

The purpose of this study was to establish whether the thiophene moiety was similarly immutable. To this end, the structures of 2-chlorothiophene and 2-bromothiophene were determined by gas phase electron diffraction. Concurrently the structure of thiophene was redetermined so that the three compounds could be compared on the basis of identical procedures.

Experimental

Samples of thiophene, 2-chlorothiophene and 2-bromothiophene were obtained commercially. Gas chromatographic analysis of the samples indicated less than one per cent impurity in each of the samples. Electron diffraction patterns were recorded on 4 × 5 inch Kodak process plates using the diffraction apparatus designed and constructed at Cornell University (Bauer & Kimura, 1962; Bauer, 1967). The patterns were recorded in the conventional convergent electron optic mode.

The temperatures of the sample reservoirs were adjusted to provide vapor pressures of 5 to 10 torr; 2-bromothiophene was maintained at room temperature, 2-chlorothiophene at 0°C and thiophene at −25°C. The ambient pressure in the diffraction apparatus varied from 1×10^{-6} to 1×10^{-5} torr during the experiments. Diffraction patterns were recorded with 65 kV electrons, at plate-to-nozzle positions of ~130 and ~260 mm. In addition, for 2-chlorothiophene and

---

* Present address: Carnegie – Mellon University, Mellon Institute, 4400 Fifth Avenue, Pittsburgh, Pa. 15213, U.S.A.

2-bromothiophene diffraction photographs were taken with 25 kV electrons at a plate-to-nozzle distance of $\sim$260 mm. These combinations gave useful diffraction patterns over $3 \le q \le 115$ Å^{-1} for 2-chlorothiophene, $4 \le q \le 119$ for 2-bromothiophene and $6 \le q \le 120$ Å^{-1} and $6 \le q \le 125$ Å^{-1} for two sets of thiophene ($q \equiv 40/\lambda \sin \Psi/2$, where Ψ is the angle between incident and scattered electron rays). The precise electron wavelengths and nozzle-to-plate distances were determined from magnesium oxide powder patterns recorded with each set of photographs. Photographs of residual gas scattering were recorded for each set of data and were substracted from the observed intensities.

The plates were scanned with a Jarrell–Ash double-beam microphotometer. They were rotated at 600 r.p.m. during the traversal across a diameter. The data for 2-chlorothiophene were obtained with a Bristol recorder while the microphotometer stage was in uniform slow motion. For the patterns of thiophene and 2-bromothiophene, the microphotometer was interfaced with a common mode differential d.c. amplifier and digital voltmeter, which at photographic densities of 0·5 or greater gave transmittance readings with a standard deviation of 0·0003. For the digitized-recording system, the microphotometer carriage is driven by a precision screw. The increment of plate advance between transmittance readings is adjustable from 10 to 1000 microns. Transmittance readings were recorded at spacings of $q/3$ and at time intervals of four seconds. The carriage was motionless while the instantaneous voltage was recorded. This system effectively eliminates correlation between adjacent readings due to finite response times of the electronic amplifying and recording system.

The transmittance readings were converted to optical density readings at integral values of q by a six-point Lagrangian interpolation formula. Since three readings were recorded for each interpolated value, the interpolation ranges for adjacent points overlap. The overlapping of adjacent interpolation ranges introduced a correlation of less than $\pm 15\%$ between adjacent points. The optical densities were corrected for non-linear darkening of the photographic plates (Hencher & Bauer, 1967), and for the fact that all areas on the flat plate are not equidistant from the scattering source.

Fig. 1 is a plot of one set of data for thiophene. To take full advantage of the precision of the digitized data, a polynomial function (sequence of points in Fig. 1) was inserted as a first approximation to the refined background curve. Calculation of the molecular intensity function, $(\pi/10)qM(q)$, and of the radial distribution function, $f(r)$, were carried out as outlined by Bonham & Bartell (1959). The X-ray atom form factors of Cromer, Larson & Waber (1963), the inelastic scattering factors of Bewilogua (1931), and the phase-shift factors fitted for computational purposes by Bonham & Ukaji (1962) were used for this analysis. The $f(r)$ curves were computed with the damping factor, γ, cited in Table 1; it was chosen so that $\exp(-\pi^2\gamma q^2_{\max}/100) = 0{\cdot}1$. After satisfactory models were obtained by matching theoretical radial distribution functions to the experimental curve, the weighted molecular intensity curve, $P(q) \times (\pi/10)qM(q)$, was fitted by a least-squares procedure as outlined by Hedberg & Iwasaki (1964).

$P(q)$ is a smooth diagonal weighting matrix chosen to qualitatively represent confidence in the experimental data. Although some correlation between adjacent points was introduced into the data by the interpolation process, a diagonal weight matrix was used to simplify the analysis. The interval between data points was chosen as integral values of q on the basis of the analysis of Murata & Morino (1966). This interval is optimum for determination of the standard deviation.

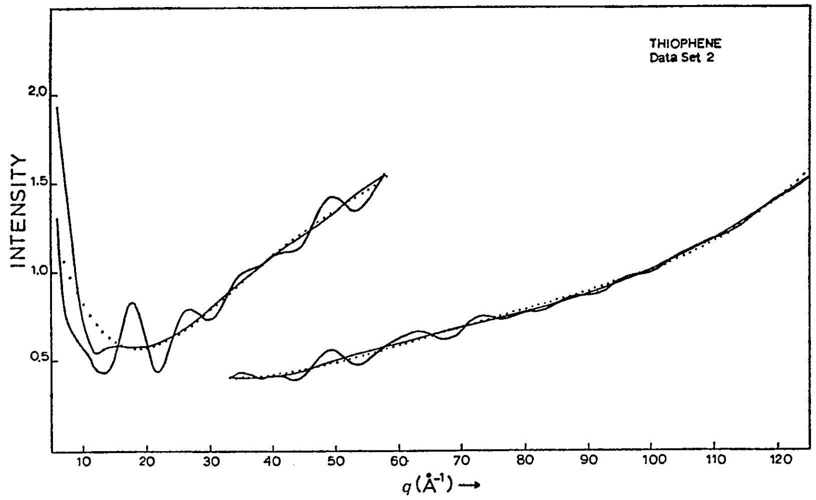

Fig. 1. The observed total intensity and refined background for data set 2 for thiophene. The dotted curves represent the polynomial background introduced to level the intensity data.

$P(q)$ is of the form:

$$P(q)=\exp[-W_1(q_1-q)],\ \text{for } q<q_1$$
$$P(q)=1,\qquad \text{for } q_1<q<q_2$$
$$P(q)=\exp[-W_2(q-q_2)],\ \text{for } q<q_2\,.$$

W_1 and W_2 were chosen such that $P(q)=0{\cdot}1$ at $q_{\min}$ and $P(q)=0{\cdot}25$ at $q_{\max}$. The magnitudes of $q_{\min}$, $q_{\max}$, q_1 and q_2 used in this reduction are listed in Table 1. Bond lengths, bond angles and mean amplitudes of vibration were fitted as parameters in the least-squares analysis.

Uncertainties for the observed parameters include standard deviations from the least-squares fit and estimated systematic errors inherent in these experiments, such as calibration of voltage and of nozzle position, sample spread at the gas nozzle, density–intensity corrections, uncertainties in atom form factors and the effects of anharmonicity. The largest of the systematic uncertainties is the determination of the voltage and of the nozzle position (*e.g.* the magnesium oxide calibration), which introduces error limits of less than 0·2% in the q scale, or an uncertainty of less than ±0·004 Å in the bond distances. Uncertainties in bond angles may be directly related to those in bond lengths while uncertainties in mean amplitudes of vibration are arbitrarily set at three times the standard deviation from the least–squares fit. For thiophene, the uncertainties of the least-squares fit were significantly smaller than those associated with the systematic errors. Thus, the error limits for thiophene were established as ±0·004 Å or three times the standard error of the optimum least-squares fit, whichever was the larger.

For 2-chloro- and 2-bromothiophene, the low symmetry of the structures leads to large correlations among the many geometric parameters fitted in the least-squares analysis. Because of this intrinsic correlation of parameters, the corresponding standard deviations are much larger than for the analogous parameters in thiophene. Thus, twice the standard deviation of the least-squares fit are adequate error limits, and these include estimates of the systematic errors for the two compounds.

Results

Thiophene

Two sets of photographs for thiophene were recorded and analyzed independently. The corresponding reduced molecular intensity curves, $(\pi/10)qM(q)$, are shown in Fig. 2 along with the fitted molecular intensity curves and the deviations for the two sets of data. Fig. 3 displays the observed and fitted radial distribution curves. The results of the least-squares analysis are listed in Table 2, as are the geometric parameters obtained by the previous investigators (Bak *et al.*, 1961; Schomaker & Pauling, 1939; Bonham & Momany

Table 1. *Ranges of observed data and limits of weighting function, $P(q)$*

Compound	$q_{\min}$ (Å^{-1})	q_1 (Å^{-1})	q_2 (Å^{-1})	$q_{\max}$ (Å^{-1})	γ
Thiophene					
Data set 1	6	15	110	120	0·00162
Data set 2	6	15	115	125	0·00149
2-Chlorothiophene	3	15	100	115	0·00176
2-Bromothiophene	4	15	105	119	0·00165

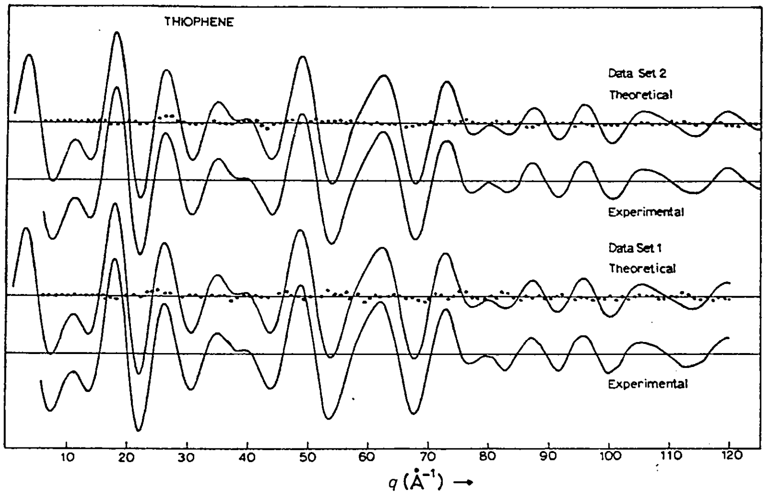

Fig. 2. Experimental molecular intensity curve and fitted theoretical curves for two sets of thiophene data. The dotted lines indicate the difference between the experimental and the calculated curves.

1963). In our least-squares analysis, twelve parameters were allowed to vary independently and convergence was obtained. The analysis indicates significant correlations between $<$CSC and $<$SCC, and $<$C(3)C(4)H and $l_{C...H}$; however, these did not prevent convergence.

Comparison of the three electron diffraction studies of thiophene show generally good agreement, with the exception of the C(3)–C(4) bond length. In the present study, this distance was treated as a dependent parameter; its length was determined by the other ring bond lengths and the fitted $<$CSC and $<$SCC. Thus, our value for C(3)–C(4) may be affected by errors present in the other fitted parameters. The average C–H bond length of 1·072 ± 0·01 Å deduced in this study is smaller than the values listed by the other investigators, and it is shorter than the C–H bond length (1·084 Å) reported for benzene (Almenningen, Bastiansen & Fernholt, 1958). However, the difference between the quoted magnitudes is less than the sums of their reported uncertainties. The amplitudes of vibration obtained in the two recent electron diffraction studies are in substantial agreement. More parameters were determined in this work since our data

Table 2. *Comparison of structure determinations of thiophene*

Parameter	Bak *et al.* (1961) (r_s)	Pauling & Schomaker (1939)	Bonham & Momany (1963)	This work (r_a) Data set 1	This work (r_a) Data set 2
Bond lengths and angles					
C–S	1·7140 ± 0·0014 Å	1·74 ± 0·03 Å	1·714 ± 0·004 Å	1·718 ± 0·004 Å	1·716 ± 0·004 Å
C=C	1·3696 ± 0·0017	1·35*	1·370 ± 0·006	1·370 ± 0·004	1·366 ± 0·004
C–C	1·4243 ± 0·0023	1·44*	1·419 ± 0·007	(1·442)	(1·442)
C–H	1·0776 ± 0·0015† 1·0805 ± 0·0014	1·09*	1·092 ± 0·008	1·075 ± 0·015	1·070 ± 0·012
∠CSC	92·16 ± 0·1°	91 ± 4°	92·2 ± 0·2°	92·0 ± 0·3°	91·8 ± 0·3°
∠SCC	111·5 ± 0·3	112 ± 3	111·4 ± 0·2	112·0 ± 0·3	112·1 ± 0·3
∠SCH	119·8 ± 0·8			121·0 ± 3·0	121·0 ± 3·0
∠C(3)C(4)H	124·25 ± 0·1			123·0 ± 6·0	117·0 ± 9·0
Amplitudes of vibration					
C–S			0·049 ± 0·005 Å	0·051 ± 0·004 Å	0·051 ± 0·004 Å
C–C			C–C 0·046*	0·042 ± 0·006	0·044 ± 0·006
			C=C 0·044*		
C–H			0·07 ± 0·01	0·077 ± 0·012	0·082 ± 0·012
C···S				0·052 ± 0·004	0·051 ± 0·006
C···H				0·070*	0·07 ± 0·03
C···C				0·050 ± 0·006	0·048 ± 0·006
Sum of squares of deviations				0·03952	0·02776
Standard deviation				0·01900	0·01556

* The value of this parameter was assumed.
† The C(2)–H bond is shorter than the C(3)–H bond.

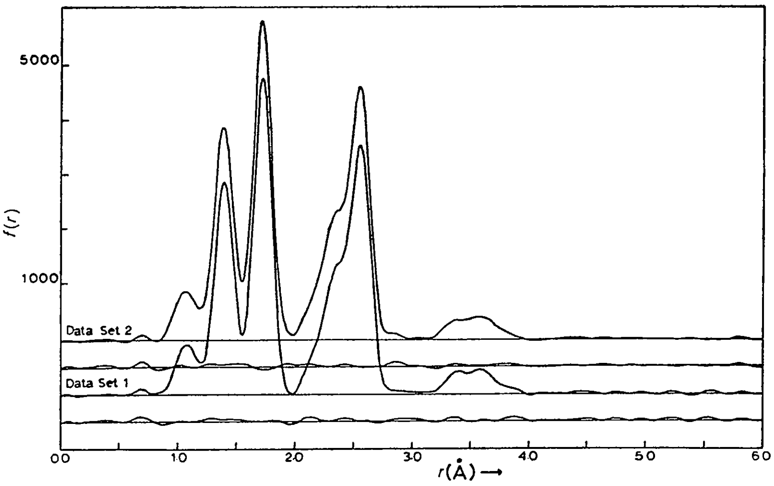

Fig. 3. The radial distribution curves for two sets of thiophene data. The deviations between the experimental $f(\mathbf{r})$ curves and the $f(\mathbf{r})$ curves calculated for the best-fitted models are shown below the experimental curves.

extended from $q=6$ to $q=125$ compared with the previous study by Bonham & Momany (1963), who used data over the interval $15 \leq q \leq 90$. The microwave analysis of Bak *et al.* (1961), in which eight isotopic species were studied, gives bond lengths (r_s values) and bond angles which are more precise than the electron diffraction results. (The least-squares program gives r_a values.)

It was assumed in this study that the thiophene molecule was planar on the basis of the small inertial defect reported in the microwave analysis. The excellent fit obtained for the diffraction data justifies this assumption.

2-*Chlorothiophene*

Preliminary analysis of the patterns indicated that the thiophene moiety was distorted by halogen substitution. Thirteen independent internal coordinates are necessary to specify the structure of the molecule, assuming the molecule is planar and that the three C–H bond lengths are equal. The number of independent amplitudes of vibration is greater. With this number of parameters, it was necessary to introduce several constraints in the least-squares analysis to obtain convergence. Final convergence was reached by constraining the amplitudes of vibration, while varying the distance parameters. Subsequently, the distance parameters were fixed at their best values, and the amplitudes of vibration were allowed to vary. Model *A* for 2-chlorothiophene was deduced in this manner. In the analysis, ten independent internal coordinates were varied, while <C(4)C(3)H, <C(3)C(4)H and <SC(5)H were fixed at 120°. After the computation converged, eight amplitudes of vibration were varied (with internal coordinates constrained) to obtain the lowest least-squares deviation. Further iterations of the least-squares program in which internal coordinates or amplitudes of vibration were alternately varied for this trial model gave no improvement for the fit. The magnitudes of these fitted parameters, along with their uncertainties, are listed under model *A*, Table 3. Fig. 4 shows the deviation of the calculated radial distribution curve for model *A* from the experimental curve. The theoretical and experimental molecular intensity curves are shown in Fig. 5.

Further least-squares analysis of the 2-chlorothio-

Table 3. *Models derived by least-squares fitting of 2-chlorothiophene and 2-bromothiophene diffraction data*

(*a*) Bond distances and angles

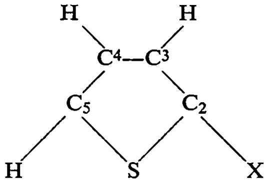

X = Cl, Br

	C_4H_3SCl		C_4H_3SBr	
	Model *A*	Model *B*	Model *A*	Model *B*
C(2)–S	1·727 ± 0·012 Å	1·709 ± 0·026 Å	1·744 ± 0·008 Å	1·668 ± 0·008 Å
C(5)–S	1·715 ± 0·012	1·742 ± 0·012	1·668 ± 0·008	1·740 ± 0·008
C(2)–C(3)	1·391 ± 0·016	1·409 ± 0·016	1·390 ± 0·014	1·465 ± 0·016
C(3)–C(4)	(1·398)	(1·361)	(1·464)	(1·393)
C(4)–C(5)	1·359 ± 0·010	1·380 ± 0·034	1·341 ± 0·014	1·339 ± 0·016
C–H	1·073 ± 0·010	1·077 ± 0·012	1·091 ± 0·026	1·089 ± 0·030
C–X	1·713 ± 0·010	1·706 ± 0·016	1·849 ± 0·008	1·850 ± 0·008
∠CSC	90·8 ± 0·3°	91·2 ± 0·3°	92·0 ± 0·6°	92·8 ± 0·8°
∠SC(5)C(4)	111·3 ± 0·6	111·1 ± 0·6	114·7 ± 1·2	111·1 ± 1·4
∠SC(2)C(3)	112·6 ± 0·8	110·9 ± 1·4	110·9 ± 1·0	111·1 ± 1·0
∠SCX	120·1 ± 0·6	121·7 ± 0·8	120·7 ± 0·6	125·2 ± 0·8

(*b*) Amplitudes of vibration

	C_4H_3SCl		C_4H_3SBr	
	Model *A*	Model *B*	Model *A*	Model *B*
C–S	0·051 ± 0·008 Å	0·047 ± 0·004 Å	0·047 ± 0·006 Å	0·047 ± 0·006 Å
C–C	0·048 ± 0·004	0·047 ± 0·004	0·047 ± 0·010	0·043 ± 0·010
C–H	0·065 ± 0·012	0·065 ± 0·010	0·08 ± 0·03	0·08 ± 0·03
C–X	0·044 ± 0·014	0·045 ± 0·006	0·047 ± 0·006	0·047 ± 0·006
S···C	0·050 ± 0·004	0·061 ± 0·004	0·050*	0·050 ± 0·006
X···C	0·067 ± 0·004	0·066 ± 0·006	0·105 ± 0·012	0·078 ± 0·016
S···X	0·066 ± 0·004	0·065 ± 0·004	0·078 ± 0·004	0·075 ± 0·004
C···C	0·046 ± 0·008	0·051 ± 0·006	0·050*	0·041 ± 0·012
Standard deviation	0·01724	0·01691	0·01578	0·01563
Sum of errors squared	0·02936	0·02711	0·02804	0·02703

* The magnitude of this parameter was assumed.

phene diffraction data indicated that model *A* was not unique. When the amplitudes of vibration were constrained to reasonable values, a nearly converged set of geometric parameters was found which differed significantly from model *A*. The least-squares solution oscillated between two very similar sets, which disagreed by much less than the calculated standard deviations for the parameters. The internal coordinates were then fixed at values intermediate between the two sets, while eight amplitudes of vibration were varied. This trial converged in less than ten cycles and the resultant solution is listed as model *B* in Table 3. The radial distribution curve for model *B* is plotted in Fig. 4; Fig. 5 presents the corresponding fitted intensity curve.

The oscillatory behavior of the least-squares solution leads to large uncertainties in the geometric parameters and large correlations between parameters. The uncertainties listed in Table 3 are twice the standard deviations for the least-squares fit. Note that the standard deviations for the geometric parameters in 2-chlorothiophene are two to ten times the standard deviations for the corresponding distances in thiophene. Large correlations were observed between C–Cl and < SC(2)C(3); $l_{\mathrm{S-C}}$ and $l_{\mathrm{C-Cl}}$; S–C(2) and S–C(5); C(2)–C(3) and C(4)–C(5).

With the exception of C(5)–S, < SCCl and $l_{\mathrm{S..C}}$, the parameters for the two models are equal to within the sum of their errors. In 2-bromothiophene, discussed below, two distinct models were also uncovered but these differ from each other by considerably more than the uncertainty of the fit. Nevertheless, these models parallel the differences between *A* and *B* in 2-chloro-

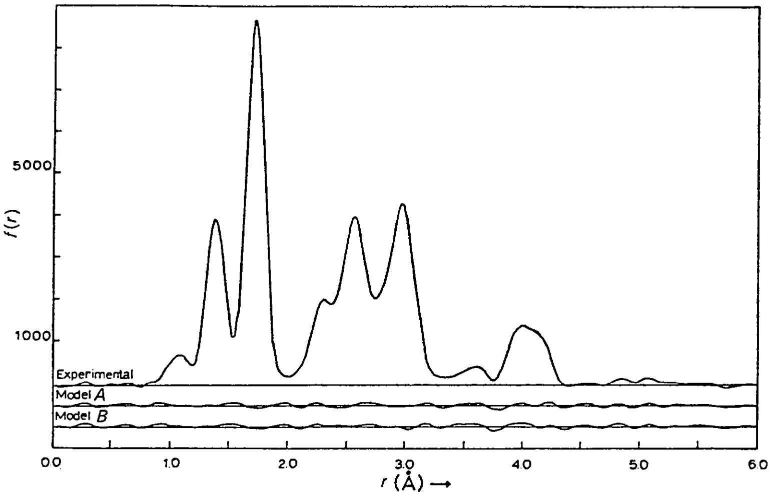

Fig. 4. Experimental radial distribution curve for 2-chlorothiophene, with deviations for the best-fitted models.

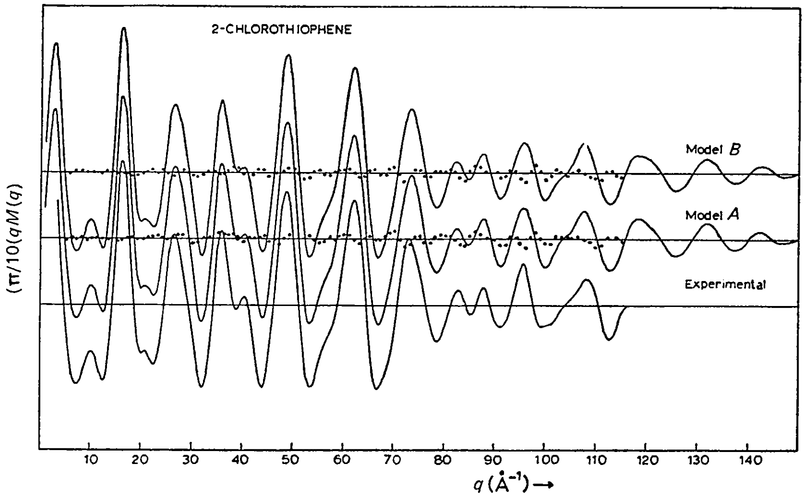

Fig. 5. Experimental molecular intensity and theoretical molecular intensity curves for the two best models of 2-chlorothiophene. The deviations between the observed and calculated curves are indicated by the sequence of points.

thiophene. Thus, models *A* and *B* for 2-chlorothiophene should be regarded as significantly different structurally although their theoretical electron diffraction patterns are indistinguishable out to $q=150$ Å^{-1}, as shown in Fig. 5.

2-*Bromothiophene*

Analysis of the 2-bromothiophene photographs followed a parallel route to that described for 2-chlorothiophene. In the least-squares analysis, the amplitudes of vibration were constrained while internal coordinates were varied. The least-squares procedure did not converge at this point but oscillated between two closely similar sets of parameters. The bond distances and angles were then fixed at values intermediate between the two while the amplitudes of vibration were varied. Then the least-squares program converged in less than ten cycles. As for 2-chlorothiophene, the diffraction data for the bromine derivative were fitted comparably well by two distinctly different models. The results of the analysis are listed in Table 3. Fig. 6 is a plot of the experimental radial distribution curve for 2-bromothiophene and the deviations of the radial distribution function for the two models. For models *A* and *B*, the experimental molecular intensity curves are compared with the calculated curves in Fig. 7; the latter show no distinguishable differences out to $q=150$ Å^{-1}.

The assumption was made that the thiophene group remained planar upon substitution. Studies to determine if the halogen atom departed from this plane indicated that the departure was less than 0·02 Å. It

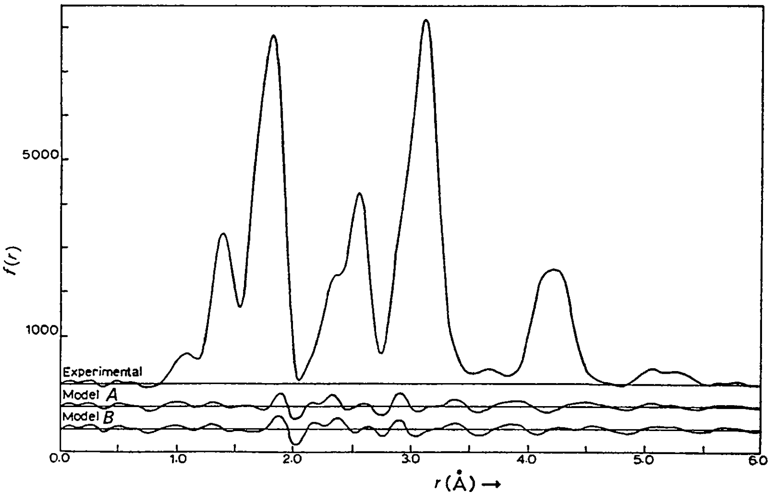

Fig. 6. Experimental radial distribution curve for 2-bromothiophene, with the deviations for the best fitting models.

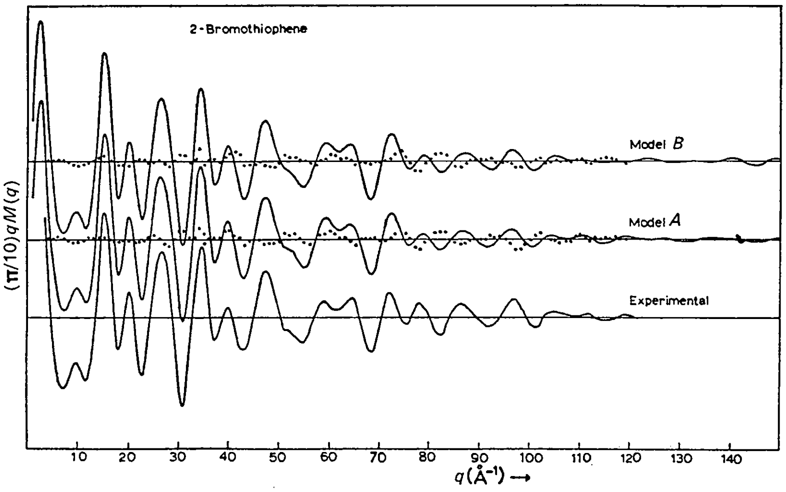

Fig. 7. Experimental molecular intensity and theoretical molecular intensity curves for the two best models of 2-bromothiophene. The deviations between the observed and calculated curves are indicated by the sequence of points.

was then assumed that the entire molecule is planar as is the case for both models *A* and *B*.

Models *A* and *B* for the halo-substituted thiophenes are structurally distinct; dimensionally they differ only in the positioning of bonded and nonbonded distances around the molecule. This is illustrated in Table 4, for 2-bromothiophene, wherein the spectrum of 33 bonded and non-bonded distances in the two models are listed. The models differ structurally in that a C–S bond (1·668 Å) is assigned to C(5)–S in model *A*, while it is C(2)–S in model *B*; a C–C bond (1·39 Å) is assigned to C(2)–C(3) in model *A*, while it is C(3)–C(4) in model *B*, *etc.* The one-dimensional projection deduced from gas phase electron diffraction parameters inherently cannot distinguish between structures which are related in this manner. The lack of uniqueness in diffraction analysis was perceived and defined more than twenty years ago by Patterson (1944) as non-congruent homometric sets of points. To establish which model best describes the structure of these substituted thiophenes, physical and chemical data other than those from diffraction must be utilized.

Table 4. *Comparison of some bonded and non-bonded distances for models A and B of* 2-*bromothiophene*

Distance type	Distance Model *A*	Distance Model *B*
⟨C–H⟩(3)	1·091 Å	1·089 Å
C–C	1·341	1·339
C–C	1·390	1·393
C–C	1·464	1·465
C–S	1·668	1·668
C–S	1·744	1·740
C–Br	1·849	1·850
⟨C···H⟩(5)	2·187	2·196
⟨C···C⟩(3)	2·341	2·339
S···H	2·407	2·472
C···S	2·544	2·549
C···S	2·586	2·585
C···Br	2·924	2·929
S···Br	3·124	3·124
Br···H	3·242	3·226
⟨C···H⟩(4)	3·389	3·398
S···H	3·617	3·619
S···H	3·653	3·646
⟨C···Br⟩(2)	4·209	4·207
Br···H	5·085	5·031
Br···H	5·287	5·328

Distances in brackets are average values for the given type. The number of distances in the average is listed in brackets. The non-bonded H···H distances were not included in this Table.

The least-squares analysis did not show large correlations between parameters. The fact that complete convergence was not obtained for the geometric parameters must be due to the close similarity in C–C bond lengths, the C–S and C–Br bond lengths, and ∠SC(2)C(3) and ∠SC(4)C(5). The curves in Figs. 6 and 7 for the bromine substituent do not show as close a fit as was obtained for thiophene or for 2-chlorothiophene. Comparison of the sum of the squares of deviations, χ_E, listed in Tables 2 and 3 for the three molecules indicates that the fit is, in fact, statistically as good for 2-bromothiophene ($\chi_E = 0{\cdot}02804$ and 0·02703) as for thiophene ($\chi_E = 0{\cdot}03952$ and 0·02776) and for 2-chlorothiophene ($\chi_E = 0{\cdot}02936$ and 0·02711). The low symmetry of the bromine derivative causes the molecular intensity curve to damp out rapidly at large *q* values. Hence, the least-squares analysis leads to a poorer fit in this region, although the general features of the observed intensity curve are reproduced.

In the analysis of 2-bromothiophene, $l_{C(2)\text{-}S}$,$l_{C(5)\text{-}S}$ and $l_{C\text{-}Br}$ were constrained to the same value. This assumption was based upon the observed $l_{C\text{-}S}$ for

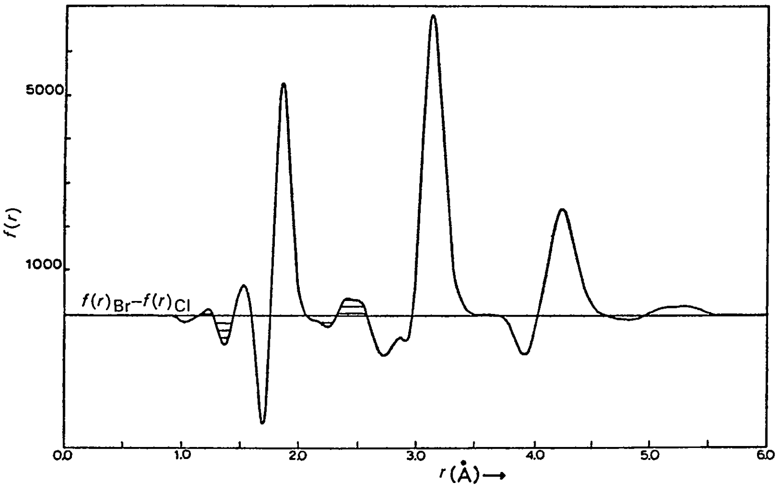

Fig. 8. The difference between the radial distribution curves for the *A* models of 2-bromothiophene and 2-chlorothiophene. The horizontal lined areas would cancel if the thiophene ring were distorted equally in the two compounds.

thiophene and $l_{\text{C–Br}}$ for 1,2-dibromobenzene (Strand, 1966). Finally trials were made in which geometrical and amplitude of vibration parameters were varied simultaneously for both the substituted thiophenes. These were unsuccessful in that they either converged very slowly or diverged, leading to unacceptable values for some parameters.

Discussion

The results of this study clearly indicate that while all three molecules are planar, the thiophene ring in the two halogenated derivatives is distorted. The distortion in the ring dimensions as a consequence of halogen substitution in the 2 position is clearly substantiated in Figs. 8 and 9. The former is a plot of the difference between the experimental radial distribution curve for model *A* of 2-chlorothiophene from that of model *A* for 2-bromothiophene. Fig. 9 shows the difference between the radial distribution curves for model *A* of the halogenated derivatives and that of thiophene. If the ring structure remained essentially unaffected by substitution, the *difference radial distribution curves* in these Figures would have been zero in the regions where they are 'lined' ($r=1{\cdot}20$ to $1{\cdot}52$ Å, $r=2{\cdot}2$ to $2{\cdot}6$ Å). In each of the three molecules, these regions correspond to bonded C–C interactions, and to nonbonded C···C and C···S interactions. Were these the same for the three molecules, there would have been cancellation of the radial distribution curves.

The remaining problem in this study is to reach a decision as to which of the two models for the halogenated derivatives best describe their structures. Fig. 10 compares some of the structural parameters for the best fitted models. In model *A* for both the chloro- and the bromo-derivatives, the bonds adjacent to the halogen atom [C(2)–S and C(2)–C(3)] are lengthened while the bonds across the ring [C(5)–S and C(4)–C(5)] are shortened relative to their values in thiophene. Conversely, in the two *B* models the bonds adjacent to the halogen atom are shortened whereas the bonds across the ring are lengthened relative to the corresponding bonds. Since the inductive effect, which presumably causes ring distortion would be similar for the two halogenated derivatives, the choice is between both models *A* or both models *B*. In that case, the proton magnetic resonance spectra reported by Gronowitz & Hoffman (1958), are pertinent. The chemical shifts for hydrogen in substituted thiophenes (relative to cyclohexane) are listed in Table 5 as abstracted from their publication. Although the p.m.r. spectra of thiophene, 2-chlorothiophene and 2-bromothiophene were not well enough resolved to permit the assignment of chemical shifts for the individual hydrogen atoms, it is apparent that inductive and mesomeric effects have perturbed the electron density of the thiophene ring in the halogenated derivatives. Additional information about such distortions may be obtained from the spectrum of 2-methoxythiophene. The $-\text{OCH}_3$ group exerts inductive effects which are similar to, but stronger than, that due to halogen atoms. Gronowitz & Hoffman (1958) interpreted the p.m.r. spectrum of 2-methoxythiophene as indicating that the 5 position in the thiophene ring has the highest electron density of the unsubstituted carbon atoms, the 3 position has the lowest density due to the electron withdrawing effects of the $-\text{OCH}_3$ group, and the 4 position is least affected by substitution. This description of the electron density distribution in the substituted thiophene is most consistent with models *A*. Mesomeric effects increase the electron density in the bonds across the ring from the halogen atoms and thus shorten them, while the electron withdrawing inductive effects of the halogen atom lengthen the adjacent bonds in the ring. Further evi-

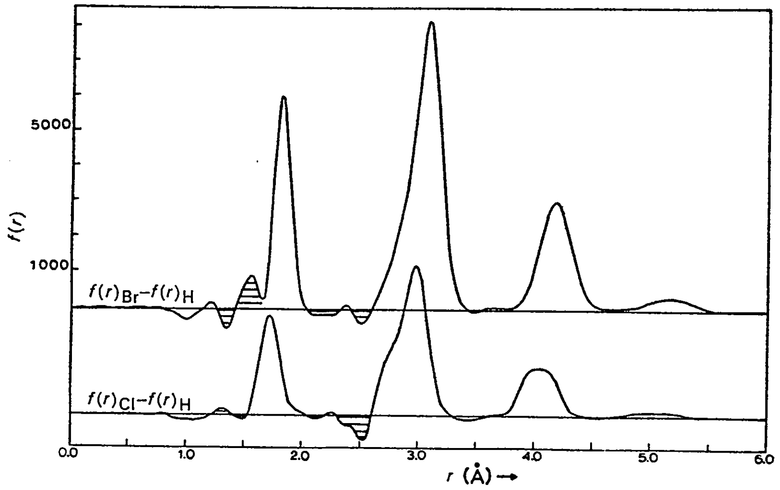

Fig. 9. The difference between the radial distribution curves for thiophene and models *A* of the halogenated derivatives. The lined areas would cancel if the thiophene ring were not distorted upon substitution.

dence for this choice of models is provided by the crystal structure of thiophene-2-carboxylic acid reported by Nardelli, Fava & Armellini (1958). In this thiophene derivative, C(2)–S (1·74 ± 0·03 Å) is longer than C(5)–S (1·72 ± 0·03 Å) and C(2)–C(3) (1·35 ± 0·02 Å) is longer than C(4)–C(5) (1·25 ± 0·04 Å). Although these C–C bond lengths are surprisingly short, the structure agrees qualitatively with models *A*.

Table 5. *Chemical shifts of hydrogen atoms in thiophene, 2-chlorothiophene and 2-bromothiophene relative to cyclohexane*

From Gronowitz & Hoffman (1958).

	Chemical shift relative to cyclohexane	Number of hydrogen atoms contributing to resonance
Thiophene	220 (p.p.m.)	4
2-Chlorothiophene	212	3
2-Bromothiophene	219	2
	210	1
2-Methoxythiophene	206	1
	199	1
	187	1

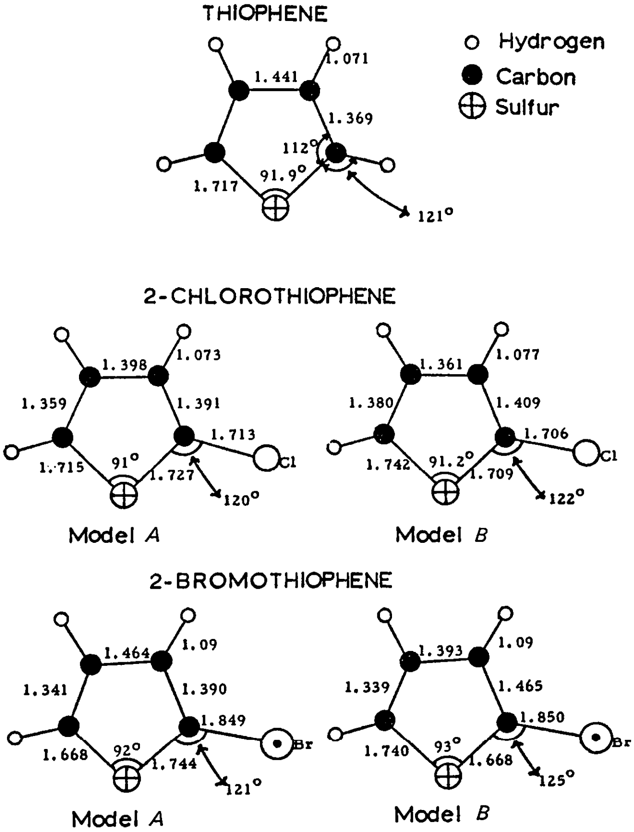

Fig. 10. Comparison of some of the geometric parameters for the best models of thiophene, 2-chlorothiophene and 2-bromothiophene.

Chemical evidence further substantiates this choice. Chlorination of 2-chlorothiophene at 50° yields 99% of 2,5-dichloro- and 1% of 2,3-dichlorothiophene (Coonradt, Hartough & Johnson, 1948) pointing to the higher reactivity of the 5 position in the 2-halogenated derivative. The only other work on substituted thiophenes which has a bearing upon the structure of these compounds is an electron diffraction study of 2,2′-bithienyl by Almenningen, Bastiansen & Svendsas (1958). However, in their analysis of the diffraction data, they *assumed* that the thiophene moiety was not distorted from C_{2v} symmetry. In the light of the above results, this assumption is questionable. The reported C–C bond length of 1·48 Å for the interannular bond indicates significant interaction which should cause a distortion of the ring structure.

It is somewhat surprising that 2-bromothiophene shows a larger distortion of the thiophene ring than does the chlorine derivative, if the distortion is based upon electron inductive effects. We have no explanation at this time. Large correlations between C–S and C–X (X = Br, Cl) bond lengths could lead to imprecision in the determination of these distances; however, the differences between the least-squares deduced C–S distances for the two halogenated derivatives are outside the most conservative interpretation of the fit of the diffraction data.

In conclusion, this investigation clearly shows that the thiophene ring is distorted from C_{2v} symmetry when halogen atoms are attached to the 2 position. Although the diffraction analysis does not distinguish between two models, other physical and chemical evidence favors that model in which the bonds adjacent to the halogen atom are lengthened, while the bonds across the ring from the halogen atoms are shortened relative to the analogous thiophene distances. The best models for thiophene and for both its derivatives are planar. Thus, in contrast to benzene, the presence of distortion in the thiophene ring upon substitution of halogen atoms, in agreement with studies of thiophene-2-carboxylic acid, 2-pyridone and 2-pyridthione (Penfold, 1953), argues that the thiophene ring is much less aromatic than is the benzene ring. It is expected that other heterocyclic rings will show distortions upon substitution in an analogous manner.

This work was supported in part by the National Science Foundation under contract No. GP-7794 and in part by the Material Science Center at Cornell University, ARPA-SD-68.

References

Akimoto, Y. (1955). *Bull. Chem. Soc. Japan*, **28**, 1.

Almenningen, A., Bastiansen, O. & Fernholt, L. (1958). *Kgl. Norske Videnskab. Selskabs Skrifter*, **3**, 3.

Almenningen, A., Bastiansen, O. & Svendsas, P. (1958). *Acta Chem. Scand.* **12**, 1671.

Bak, B., Christensen, D., Hansen-Nygaard, L. & Rastrup-Andersen, J. (1961). *J. Mol. Spectr.* **7**, 58.

BAUER, S. H. (1967). *Electron Diffraction Studies at High Temperatures*. Report Nonr-401(41), Project NRO92-504, ARPA order No. 23-53.
BAUER, S. H., KATADA, K. & KIMURA, K. (1968). *Structural Chemistry and Molecular Biology*, Ed. A. RICH and N. DAVIDSON, p. 653. San Francisco: Freeman.
BAUER, S. H. & KIMURA, K. (1962). *J. Phys. Soc. Japan*, **17**, 300.
BEWILOGUA, L. (1931). *Phys. Z.* **32**, 740.
BONHAM, R. A. & BARTELL, L. S. (1959). *J. Chem. Phys.* **31**, 702.
BONHAM, R. A. & MOMANY, F. A. (1963). *J. Phys. Chem.* **67**, 2474.
BONHAM, R. A. & UKAJI, T. (1962). *J. Chem. Phys.* **36**, 72.
COONRADT, H. L., HARTOUGH, H. D. & JOHNSON, G. C. (1948). *J. Amer. Chem. Soc.* **70**, 2564.
CROMER, D. T., LARSON, A. C. & WABER, J. T. (1963). Los Alamos Scientific Laboratory Reports, LA-2987.
GRONOWITZ, S. & HOFFMAN, R. A. (1958). *Ark. Kemi*, **13**, 279.
HEDBERG, K. & IWASAKI, M. (1964). *Acta Cryst.* **17**, 529.
HENCHER, J. L. & BAUER, S. H. (1967). *J. Amer. Chem. Soc.* **89**, 522.
KIMURA, K. & KUBO, M. (1960). *J. Chem. Phys.* **32**, 1776.
LANCASTER, J. E. & STOICHEFF, B. B. (1956). *Canad. J. Phys.* **34**, 1016.
LANGSETH, A. & STOICHEFF, B. P. (1956). *Canad. J. Phys.* **34**, 350.
LONGUET-HIGGINS, H. C. (1949). *Trans. Faraday Soc.* **45**, 174.
MURATA, Y. & MORINO, Y. (1966). *Acta Cryst.* **20**, 605.
NARDELLI, M., FAVA, G. & ARMELLINI, L. (1958). *Ric. Sci.* **28**, 383; *Structure Reports*, Ed. W. B. PEARSON. Vol. 22, p. 770. Utrecht: Oosthoek.
PATTERSON, A. L. (1944). *Phys. Rev.* **65**, 195.
PENFOLD, B. R. (1953). *Acta Cryst.* **6**, 591, 707.
SCHOMAKER, V. & PAULING, L. (1939). *J. Amer. Chem. Soc.* **69**, 1769.
STRAND, T. G. (1966). *J. Chem. Phys.* **44**, 1661.

Acta Cryst. (1970). B**26**, 1020

CuWO$_4$, a Distorted Wolframite-Type Structure

BY LARS KIHLBORG AND ELIZABETH GEBERT*

Institute of Inorganic and Physical Chemistry, University of Stockholm, S-104 05 *Stockholm, Sweden*

(*Received* 17 *July* 1969)

The crystal structure of CuWO$_4$, previously reported by the authors to be of a distorted wolframite type, has been refined from single-crystal X-ray diffractometer data. The least-squares procedure including anisotropic thermal parameters resulted in a conventional $R=0{\cdot}029$. The structure is triclinic, space group $P\bar{1}$, with unit-cell dimensions $a=4{\cdot}7026\,(\pm 6)$, $b=5{\cdot}8389\,(\pm 7)$, $c=4{\cdot}8784\,(\pm 6)$ Å, $\alpha=91{\cdot}677\,(\pm 9)$, $\beta=92{\cdot}469\,(\pm 7)$ and $\gamma=82{\cdot}805\,(\pm 10)°$. The copper atom is surrounded by six oxygen atoms, four of these in an approximately square planar configuration and the remaining two at a longer distance completing an elongated octahedron. The tungsten atom is located within a slightly distorted octahedron but is considerably displaced from its centre. Interatomic distances and angles are given. The refinement gave no evidence for oxygen deficiency and new density measurements have given values which, although still somewhat low, are closer to that expected for stoichiometric composition than was the previously reported value.

Introduction

In a previous communication from this Institute we reported a preliminary investigation of the crystal structure of copper tungstate, CuWO$_4$, which we found to be a distorted version of the wolframite type (Gebert & Kihlborg, 1967). Density measurements led us to believe that our samples were strongly oxygen deficient; hence we preferred to give the formula as CuWO$_{4-x}$. The study was based on photographically recorded X-ray diffraction intensities obtained from a twinned crystal. The relatively poor quality of the data limited the degree of accuracy that could be achieved. The final R value was 0·20.

When the preliminary investigation had reached a final stage we found an untwinned single crystal of the phase. This paper reports a refinement of the structure based on diffractometer data obtained from this crystal.

Experimental

The crystal was selected from a sample prepared by heating an equimolar mixture of CuO and WO$_3$ (reagent grade) in an evacuated platinum tube for 4 days at 800°C. The preparation did not appear homogeneous under the microscope; it contained both light yellow, well-developed crystals and amber-coloured pieces with a glassy appearence. Its powder pattern, however, showed only the lines characteristic for CuWO$_{4-x}$ (Gebert & Kihlborg, 1967) and single-crystal photographs revealed that both types of crys-

---

* On leave from Argonne National Laboratory, Argonne, Illinois, U.S.A.